ELSEVIER

Earth and Planetary Science Letters 177 (2000) 163–176

EPSL

www.elsevier.com/locate/epsl

Fault finiteness and initiation of dynamic shear instability

Cristian Dascalu [a,b,*], Ioan R. Ionescu [a], Michel Campillo [c]

[a] *Laboratoire de Mathématiques, Université de Savoie, 73376 Le Bourget-du-Lac Cedex, France*
[b] *Institute of Applied Mathematics, Romanian Academy, P.O. Box 122, 70700 Bucharest, Romania*
[c] *Laboratoire de Géophysique Interne, Université Joseph Fourier, P.O. Box 53X, 38041 Grenoble Cedex, France*

Received 5 May 1999; received in revised form 28 January 2000; accepted 10 February 2000

Abstract

We study the initiation of slip instabilities of a finite fault in a homogeneous linear elastic space. We consider the antiplane unstable shearing under a slip-dependent friction law with a constant weakening rate. We attack the problem by spectral analysis. We concentrate our attention on the case of long initiation, i.e. small positive eigenvalues. A static analysis of stability is presented for the nondimensional problem. Using an integral equation method we determine the first (nondimensional) eigenvalue which depends only on the geometry of the problem. In connection with the weakening rate and the fault length this (universal) constant determines the range of instability for the dynamic problem. We give the exact limiting value of the length of an unstable fault for a given friction law. By means of a spectral expansion we define the 'dominant part' of the unstable dynamic solution, characterized by an exponential time growth. For the long-term evolution of the initiation phase we reduce the dynamic eigenvalue problem to a hypersingular integral equation to compute the unstable eigenfunctions. We use the expression of the dominant part to deduce an approximate formula for the duration of the initiation phase. Finally, some numerical tests are performed. We give the numerical values for the first eigenfunction. The dependence of the first eigenvalue and the duration of the initiation on the weakening rate are pointed out. The results are compared with those for the full solution computed with a finite-differences scheme. These results suggest that a very simple friction law could imply a broad range of duration of initiation. They show the fundamental role played by the limited extent of the potentially slipping patch in the triggering of an unstable rupture event.

Keywords: faults; slip rates; eigenvalues; shear; rupture

1. Introduction

We define the initiation phase as the period between a perturbation of the mechanical conditions of a fault system and the onset of rupture propagation which is associated with wave radiation. We do not discuss here the origin of the perturbation. It may be for example the effect of a distant earthquake or a local small variation of strain due to a rapid change of fluid pressure. Iio [9] and Ellsworth and Beroza [6] observed a weak slow increase in ground motion before the strong seismic pulse associated with the propagating rupture front. They interpreted this signal as a marker of the initiation phase. However, the characteristic time scale of this observation is typically of the order of 1 s. A much longer initiation phase

* Corresponding author.
E-mail: Cristian.Dascalu@univ-savoie.fr

0012-821X/00/$ – see front matter
PII: S0012-821X(00)00055-8

can be expected during which the slip accelerates exponentially. The present-day instruments can only detect the very last stage associated with large enough slip velocity.

On the other hand, one can observe that an earthquake can be triggered by another one with various large delays. A typical example is the 3 h delay between the Landers and Big Bear earthquakes of 1992, but the delay may be much larger (see Harris [8] for a review). It is also established that the time distribution of seismicity has no correlation with the stress changes associated with the tides (see Vidale et al. [14]). This suggests that the delay between a perturbation of stress and the onset of rupture propagation is variable and may be at least as large as the period of the tides. Do such long initiation times preclude using simple elastic models? Do they imply that one has to consider complex ad-hoc friction laws?

To provide some elements to answer these questions, we studied the range of initiation duration expected for simple models of fault. The case of the single fault which is treated here is a building block for a more developed model of fault. The complete understanding of the physics of its spontaneous rupture is therefore critical for the set-up of dynamic fault models. We investigated the domain of evolution between the long-term quasi-static evolution governed by the slow external driving (plate) motion and the extremely rapid slip in the rupture propagation stage. This intermediate time scale sets specific difficulties. The dynamic aspect of the problem cannot be ignored during the onset of the instability, that is the period of continuous acceleration of the slip process. At the same time, the long duration of initiation is not compatible with the standard numerical techniques used to deal with rupture dynamics. We propose a spectral resolution of the problem that takes advantage of the very fundamental properties of the solution of the complete problem in the initiation stage.

We consider an elastic body with a fault characterized by a slip-dependent friction law. Campillo and Ionescu [3,10] studied a slip weakening law deduced from laboratory experiments (see for instance [12]). They considered in [3] a piecewise linear version of the friction law and an infinite fault. They derived the generic form of the unstable behavior in the initiation phase and gave the characteristic length l_f associated with the friction law. In [10] they studied a nonlinear weakening and showed the determinant role of the initial weakening for the duration of initiation, which is only weakly sensitive to the critical slip for a given the initial weakening rate. They also showed numerically that the finiteness of the fault strongly affects the duration of initiation when the fault length $2a$ is of the same order as a characteristic length associated with the friction law l_f. However, the numerical simulation does not make it possible to investigate the behavior of the fault when $2a$ is equal to or less than l_f, since these conditions lead to a very long duration of evolution that cannot be handled with the finite difference technique. As a consequence, the minimum fault length $2a_c$ required for an instability to develop cannot be evaluated numerically. Its order of magnitude is known only by a static stability analysis based on the analogy with a block slider system. The goal of the present paper was to find a theoretical manner of dealing with the dynamic evolution of the system when a is close to a_c, that is at the limit between the stable and unstable behaviors.

After the formal statement of the nondimensional dynamic problem, we present its spectral expansion. We emphasize the role of the static stability analysis to characterize the transition between stable and unstable behaviors. This transition is associated with a (universal) value of a new nondimensional parameter β which emerges from the spectral analysis of the problem. We compute the eigenfunctions and give an approximate formula for the time of initiation. Finally we present numerical tests demonstrating the accuracy of our approach.

2. Problem statement

We consider the antiplane shearing on a finite fault $y=0$, $|x|<a$ of length $2a$, denoted by Γ_f, in a homogeneous linear elastic space. The contact on the fault is described by a slip-dependent friction law. We assume that the displacement field is

0 in directions Ox and Oy and that u_z does not depend on z. The displacement is therefore denoted simply by $w(t,x,y)$. The elastic medium has a shear rigidity G, a density ρ and a shear velocity $c=\sqrt{G/\rho}$. The nonvanishing shear stress components are $\sigma_{zx}=\tau_x^\infty+G\partial_x w(t,x,y)$ and $\sigma_{zy}=\tau_y^\infty+G\partial_y w(t,x,y)$, and the normal stress on the fault plane is $\sigma_{yy}=-S$ $(S>0)$.

The equation of motion is:

$$\frac{\partial^2 w}{\partial t^2}(t,x,y)=c^2\nabla^2 w(t,x,y) \tag{1}$$

for $t>0$ and (x,y) outside the fault Γ_f. The boundary conditions on Γ_f are:

$$\sigma_{zy}(t,x,0+)=\sigma_{zy}(t,x,0-),\ |x|<a \tag{2}$$

$$\sigma_{zy}(t,x,0)=$$

$$\mu(\delta w(t,x))S\ \text{sign}\left(\frac{\partial \delta w}{\partial t}(t,x)\right),\ |x|<a \tag{3}$$

if $\partial_t\delta w(t,x)\neq 0$ and:

$$|\sigma_{zy}(t,x,0)|\leq\mu(\delta w(t,x))S,\ |x|<a \tag{4}$$

if $\partial_t\delta w(t,x)=0$, where $\delta w(t,x)=1/2(w(t,x,0+)-w(t,x,0-))$ is the half of the relative slip and $\mu(\delta w)$ is the coefficient of friction on the fault.

The initial conditions are denoted by w_0 and w_1, that is:

$$w(0,x,y)=w_0(x,y),\ \frac{\partial w}{\partial t}(0,x,y)=w_1(x,y) \tag{5}$$

Since our intention is to study the evolution of the elastic system near an unstable equilibrium position, we shall suppose that $\tau_y^\infty=S\mu_s$, where $\mu_s=\mu(0)$ is the static value of the friction coefficient on the fault. We remark that taking w as a constant satisfies Eqs. 1–4; hence $w\equiv 0$ is a metastable equilibrium position, and w_0, w_1 may be considered small perturbations of the equilibrium. We shall suppose that the friction law has the form of a piecewise linear function:

$$\mu(\delta w)=\mu_s-\frac{\mu_s-\mu_d}{L_c}\delta w,\ \delta w\leq L_c \tag{6}$$

$$\mu(\delta w)=\mu_d,\ \delta w>L_c \tag{7}$$

where μ_s and μ_d $(\mu_s>\mu_d)$ are the static and dynamic friction coefficients, and L_c is the critical slip. Let us assume in the following that the slip δw and the slip rate $\partial_t\delta w$ are non-negative. Bearing in mind that we deal with a homogeneous fault plane and with the evolution of one initial pulse, we may put (for symmetry reasons) $w(t,x,y)=-w(t,x,-y)$, hence we consider only one half-space $y>0$ in Eq. 1 and Eq. 5. With these assumptions, Eqs. 2–4 become:

$$w(t,x,0)=0,\ \text{for}\ |x|\geq a \tag{8}$$

$$\frac{\partial w}{\partial y}(t,x,0)=-\alpha w(t,x,0+)\ \text{if}$$

$$w(t,x,0)\leq L_c,\ \text{for}\ |x|<a \tag{9}$$

$$\frac{\partial w}{\partial y}(t,x,0)=-\alpha L_c\ \text{if}\ w(t,x,0)>L_c,\ \text{for}\ |x|<a \tag{10}$$

where α is a parameter which has the dimension of a wavenumber (m^{-1}) and which will play an important role in our further analysis. The value α is given by:

$$\alpha=\frac{(\mu_s-\mu_d)S}{GL_c} \tag{11}$$

It is important to note that α is proportional to the weakening rate. Note that this parameter was denoted by α_c in the case of the infinite fault (see [3]) when it represents a characteristic (critical) wave number. It no longer plays such a role in the present discussion on a finite fault.

3. Nondimensional problem and its spectral expansion

Since the initial perturbation (w_0,w_1) of the equilibrium state $w\equiv 0$ is small, we have $w(t,x,0+)\leq L_c$ for $t\in[0,T_c]$ for all x, where T_c is a critical time for which the slip on the fault reaches the critical value L_c at least at one point, that is, $\sup_{x\in R}w(T_c,x,0+)=L_c$. Hence for a first period $[0,T_c]$, called in what follows the initiation

period, we deal with a linear initial and boundary value problem (Eqs. 1, 5 and 9).

In order to obtain some universal entities (depending only on the geometrical configuration) to characterize the stability of the above problem, we give here its nondimensional formulation. If we put:

$$x_1 =: \frac{x}{a},\ x_2 =: \frac{y}{a}$$

and we introduce the following nondimensional constant:

$$\beta = a\alpha = a\frac{(\mu_s - \mu_d)S}{GL_c} \tag{12}$$

then from Eqs. 1, 5 and 9 we deduce:

$$\frac{\partial^2 w}{\partial t^2}(t, x_1, x_2) = \frac{c^2}{a^2}\nabla^2 w(t, x_1, x_2) \tag{13}$$

$$w(t, x_1, 0) = 0, \text{ for } |x|_1 \geq 1 \tag{14}$$

$$\frac{\partial w}{\partial x_2}(t, x_1, 0) = -\beta w(t, x_1, 0), \text{ for } |x_1| < 1 \tag{15}$$

$$w(0, x_1, x_2) = w_0(x_1, x_2),\ \frac{\partial w}{\partial t}(0, x_1, x_2) = w_1(x_1, x_2) \tag{16}$$

Let us consider the following eigenvalue problem connected to Eqs. 13–16: find Φ: $R \times R_+ \to R$ and λ^2 such that:

$$\int_{-\infty}^{+\infty}\int_{0}^{+\infty} \Phi^2(x_1, x_2)\mathrm{d}x_1\mathrm{d}x_2 = 1$$

and:

$$\nabla^2\Phi(x_1, x_2) = \lambda^2\Phi(x_1, x_2), \text{ for } x_2 > 0 \tag{17}$$

$$\Phi(x_1, 0) = 0, \text{ for } |x|_1 \geq 1 \tag{18}$$

$$\frac{\partial}{\partial x_2}\Phi(x_1, 0) = -\beta\Phi(x_1, 0), \text{ for } |x_1| < 1 \tag{19}$$

Since we deal with a symmetric operator we have real-valued eigenvalues λ^2, i.e. λ is real or purely imaginary. Since the boundary conditions (Eqs. 18 and 19) are included in the definition of the operator (see Ionescu and Paumier [11] for a precise functional framework) this symmetry property is specific to the slip-dependent friction law used here. Let us denote by (λ_n^2, Φ_n) the associated eigenvalues and the eigenfunctions of Eqs. 17–19. Bearing in mind the above notations, one can verify (by simple calculation) that the solution of Eqs. 13–16 can be generically written (in its spectral expansion) as:

$$w(t, x_1, x_2) = \sum_{n=0}^{\infty}[\cosh(c\lambda_n t/a)W_n^0 + a\frac{\sinh(c\lambda_n t/a)}{c\lambda_n}W_n^1]\Phi_n(x_1, x_2), \text{ for } x_2 > 0 \tag{20}$$

where:

$$W_n^0 = \int_{-\infty}^{+\infty}\int_{0}^{+\infty} \Phi_n(x_1, x_2)w_0(x_1, x_2)\mathrm{d}x_1\mathrm{d}x_2 \tag{21}$$

$$W_n^1 = \int_{-\infty}^{+\infty}\int_{0}^{+\infty} \Phi_n(x_1, x_2)w_1(x_1, x_2)\mathrm{d}x_1\mathrm{d}x_2 \tag{22}$$

are the projections of the initial data on the eigenfunctions. Let N be such that:

$$\lambda_0^2 > \lambda_1^2 > \ldots > \lambda_{N-1}^2 > 0 > \lambda_N^2 > \ldots$$

We remark that the part of the solution associated with positive eigenvalues λ^2 will have an exponential growth with time. Hence, after a while this part will completely dominate the other part which has a wave-type evolution. This behavior is the expression of the instability caused by the slip weakening friction law. This is why we put:

$$w = w^d + w^w$$

where w^d is the 'dominant part' and w^w is the 'wave part', given by:

$$w^d(t, x_1, x_2) = \sum_{n=0}^{N-1}[\cosh(c|\lambda_n|t/a)W_n^0 + a\frac{\sinh(c|\lambda_n|t/a)}{c|\lambda_n|}W_n^1]\Phi_n(x_1, x_2) \tag{23}$$

$$w^{w}(t,x_1,x_2)=\sum_{n=N}^{\infty}[\cos(c|\lambda_n|t/a)W_n^0+$$

$$a\frac{\sin(c|\lambda_n|t/a)}{c|\lambda_n|}W_n^1]\Phi_n(x_1,x_2) \quad (24)$$

The use of the expression of the dominant part leads to a solution in which the perturbation has been severely smoothed by the finite wavenumber integration. The propagative terms are rapidly negligible and the shape of the slip distribution is almost perfectly described by the dominant part. This was already noticed by Campillo and Ionescu [3] in the case of the infinite fault.

4. Stability analysis

One can easily see that $w\equiv 0$ is a stable position if $\lambda_0^2<0$ (i.e. $N=0$). In this case the dominant part w^d vanishes and the system has a stable behavior. Hence it is important to obtain a simple condition on β which determines the positiveness of the eigenvalues λ^2. Since β is nondimensional such a condition depends only on the geometry of the domain and it completely characterizes the stability. The numerical simulation does not permit investigation of the behavior of the fault when λ_0 is small and greater than 0, since these conditions lead to very long durations of evolution that we are not able to handle with the finite-differences technique. As a consequence, the minimum fault length required for an instability to develop cannot be evaluated numerically. Its order of magnitude is known only by a static stability analysis based on the analogy with a block slider system. In order to obtain a more precise evaluation a sharper stability analysis has to be considered (see Ionescu and Paumier [11] for some general results in the case of a finite domain).

In order to perform a stability analysis let us introduce the eigenvalue problem corresponding to the static case: find φ: $R\times R_+\to R$ and β such that:

$$\int_{-\infty}^{+\infty}\int_{0}^{+\infty}\varphi^2(x_1,x_2)\mathrm{d}x_1\mathrm{d}x_2=1$$

and:

$$\nabla^2\varphi(x_1,x_2)=0, \text{ for } x_2>0 \quad (25)$$

$$\varphi(x_1,0)=0, \text{ for } |x_1|\geq 1 \quad (26)$$

$$\partial_{x_2}\varphi(x_1,0)=-\beta\varphi(x_1,0), \text{ for } |x_1|<1 \quad (27)$$

This problem has a sequence of positive eigenvalues $0<\beta_0<\beta_1<\ldots$ with:

$$\lim_{n\to\infty}\beta_n=+\infty.$$

The eigenvalues β_k may be viewed in connection with the dynamic eigenvalue problem (Eqs. 17–19). Indeed, they correspond to the intersection points of the increasing curves $\beta\to\lambda_k^2(\beta)$ with the axis $\lambda^2=0$ (i.e. $\lambda_k^2(\beta_k)=0$). Such functions are generically represented in Fig. 1.

The first eigenvalue β_0 has a major significance in the static stability analysis: if $\beta<\beta_0$ then $\lambda_0^2<0$, i.e.:

$$\text{if } a\frac{(\mu_s-\mu_d)S}{GL_c}=\beta<\beta_0 \text{ then } w\equiv 0 \text{ is stable} \quad (28)$$

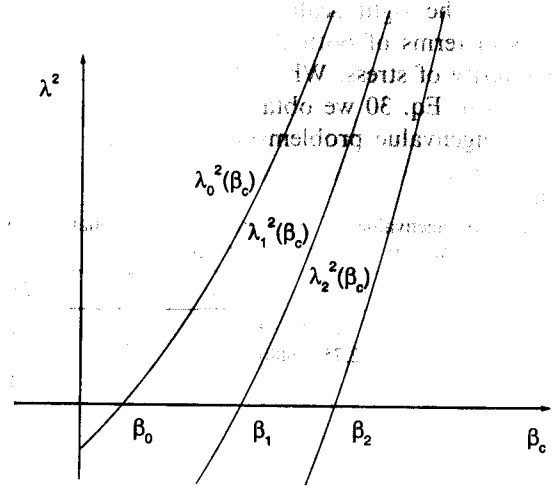

Fig. 1. The generic representation of the first three eigenvalues $\lambda_0^2=\lambda_0^2(\beta)$, $\lambda_1^2=\lambda_1^2(\beta)$ and $\lambda_3^2=\lambda_3^2(\beta)$ versus the nondimensional weakening parameter β. Note the intersection with the axis $\lambda^2=0$ on the eigenvalues β_0, β_1, β_2 of the static problem.

Moreover, if $\beta > \beta_0$ one obtains (see Fig. 1) the number N of positive eigenvalues λ^2 contained in the expression of the dominant part, i.e.:

$$\text{if } \beta \in (\beta_{N-1}, \beta_N) \text{ then } \lambda_0^2 > \lambda_1^2 > \ldots > \lambda_{N-1}^2 > 0 > \lambda_N^2 > \ldots \tag{29}$$

The sequence $(\beta_k)_{k\geq 0}$ plays an important role in the stability of the dynamic solution and the structure of the dominant part. The aim of this section is to determine the numerical values of β_k.

In Appendix A we have reduced the problem of Eqs. 25–27 to the following hypersingular integral equation for $\varphi(x_1,0)$:

$$\varphi(x_1,0) = \frac{1}{\beta\pi} PV \int_{-1}^{1} \frac{\partial_s \varphi(s,0)}{x_1 - s} ds \quad |x_1| < 1 \tag{30}$$

where the integral is taken in the Cauchy principal value sense. Note that Eq. 30 is similar to the Prandtl equation for the compressible case in aerodynamics (see for instance [4,5]). To solve Eq. 30 we seek a solution of the form:

$$\varphi(x_1,0) = \sum_{n=1}^{\infty} u_n \sin(n \arccos(x_1)) \tag{31}$$

Let us remark that each term of this expansion contains the right scaling behavior at the fault edges in terms of both the displacement and the singularity of stress. When this expression is substituted in Eq. 30 we obtain the following generalized eigenvalue problem (see the details in Appendix A) involving the infinite matrices A and B:

$$\beta \sum_{n=1}^{\infty} A_{kn} u_n = \sum_{n=1}^{\infty} B_{kn} u_n, \quad k = 1, 2, \ldots \tag{32}$$

where:

$$A_{kn} = -\frac{2kn(1+(-1)^{k+n})}{((k-n)^2-1)((k+n)^2-1)}$$

$$(1-\delta_{n,k-1})(1-\delta_{n,k+1}), \quad B_{kn} = \frac{n\pi}{2}\delta_{k,n} \tag{33}$$

By retaining the first M terms in the series in Eq. 32 we obtain a 'generalized eigenproblem' for β^M with the eigenvectors $(u_n^M)_{n=1,M}$, i.e.:

$$\beta^M A^M u^M = B^M u^M \tag{34}$$

where $A_{ij}^M = A_{kn}$ and $B_{kn}^M = B_{kn}$ for $1 \leq k, n \leq M$. This problem was numerically solved for $M = 20$, $M = 100$ and $M = 1000$ and the first 10 eigenvalues are given in Table 1.

The constant β_0 depends only on the geometry of the antiplane problem with a finite fault and it is independent of all physical entities involved in our problem. We remark that the smallest eigenvalue was found as:

$$\beta_0 = 1.15777388 \tag{35}$$

This nondimensional parameter gives quantitatively the limit between the stable ($\beta < \beta_0$) and

Table 1
The first 10 eigenvalues of the static nondimensional problem (Eqs. 25–27) computed from the truncated algebraic eigenproblem (Eq. 34) for $M = 20$, $M = 100$ and $M = 1000$

	$M = 20$	$M = 100$	$M = 1000$
β_0	1.15777389	1.15777388	1.15777388
β_1	2.75475480	2.75475474	2.75475474
β_2	4.31680136	4.31680107	4.31680107
β_3	5.89214801	5.89214747	5.89214747
β_4	7.46017712	7.46017574	7.46017574
β_5	9.03285448	9.03285269	9.03285269
β_6	10.60229691	10.60229310	10.60229310
β_7	12.17412302	12.17411826	12.17411826
β_8	13.74413789	13.74410906	13.74410906
β_9	15.31570893	15.31555500	15.31555500

Note that there is no variation of the eigenvalues at this level of accuracy.

unstable ($\beta > \beta_0$) behaviors of the fault. For each representative physical quantity which is included in the nondimensional parameter β (the stress drop $(\mu_s - \mu_d)S$, the friction weakening slope $(\mu_s - \mu_d)S/L_c$, the interface stiffness G/a, the fault half length a, the elastic bulk modulus G, etc.) we can define a 'critical' value. For instance, according to Eq. 28 the minimum half length a_c of an unstable fault is:

$$a_c = \frac{\beta_0}{\alpha} = \frac{\beta_0 G L_c}{(\mu_s - \mu_d)S} \tag{36}$$

This critical fault length for unstable behavior is a concept very different from that of critical crack length of a propagating crack as developed by Palmer and Rice [13] or Andrews [1]. The critical fault length defined here refers to the development of instability on a heterogeneous fault surface while the critical crack length is related to the energy balance of a propagating crack on a homogeneous fault.

5. Spectral analysis of initiation

During the initiation phase the essential behavior of the solution w of Eqs. 13–16 is given by its dominant part w^d. In order to compute w^d we have to determine the eigenvalues λ_n and the eigenfunctions Φ_n, for $n = 0, N$ from Eqs. 17–19. This is the objective of this section. These results will be used in the next section to compute the long-term evolution of the slip during the initiation phase. Such a ??long initiation period can be obtained only for small values of λ. This assumption, i.e.:

$$|\lambda| \ll 1$$

will be adopted in what follows.

To study the problem in Eqs. 17–19 we employ a technique similar to that in the static case. Since in the expression of the dominant part it appears $|\lambda|$ for λ real-valued we seek only positive λ in what follows. The details of calculus are presented in Appendix B. We have deduced the hypersingular integral equation for $\Phi(x_1,0)$:

$$\Phi(x_1,0) = -\frac{\lambda}{\pi\beta} FP \int_{-1}^{1} \Phi(s,0) \frac{K_1(\lambda|s-x_1|)}{|s-x_1|} ds, \quad |x_1| < 1 \tag{37}$$

where K_1 is the modified Bessel function of the second kind and the integral is taken in the finite-part sense (see for instance [7]). For small values of λ (i.e. $\lambda \ll 1$), we can approximate Eq. 37 by:

$$\pi\beta\,\Phi(x_1,0) = PV \int_{-1}^{1} \frac{\partial_s \Phi(s,0) ds}{x_1 - s} - \lambda^2 \int_{-1}^{1} \Phi(s,0) \ln(\lambda|s-x_1|) ds \tag{38}$$

with $|x_1| < 1$ and the integral is taken in the principal value sense. We seek a solution for Eq. 38 of the form:

$$\Phi(x_1,0) = \sum_{n=1}^{\infty} U_n \sin(n \arccos(x_1)) \tag{39}$$

which implies the following generalized eigenvalue problem involving infinite matrices:

$$\beta \sum_{n=1}^{\infty} A_{kn} U_n = \sum_{n=1}^{\infty} (B_{kn} + C_{kn}(\lambda)) U_n, \quad k = 1, 2, \ldots \tag{40}$$

with A_{kn}, B_{kn} given by Eq. 33 and:

$$C_{kn}(\lambda) = \frac{\pi\lambda^2 \ln\lambda}{4} \delta_{n,1}\delta_{k,1} - \frac{\pi\lambda^2}{16} (\delta_{k,3} - (1 + 4\ln 2)\delta_{k,1})\delta_{n,1} - \frac{\pi\lambda^2}{8(n^2-1)}(1-\delta_{n,3}) [(n-1)\delta_{k,n+2} + (n+1)\delta_{k,n-2} - 2n\delta_{k,n}] \tag{41}$$

Our objective is to determine $\lambda(\beta)$ and $U_n(\beta)$, $n = 1,2,\ldots$. The form (Eq. 40) of the system suggests an analysis of the eigenvalue problem with β as the eigenvalue and λ as a parameter. Such a technique will finally provide the values of $\lambda(\beta)$ and the corresponding eigenvectors $U_n(\beta)$.

As in the static analysis, we retain the first M terms in the series (Eq. 40). Since for the description of the initiation process only the first value of λ, denoted λ_0, is relevant, we shall determine numerically λ_0 as a function of β and the corresponding eigenvector $U_n^0(\beta)$. Then, by Eq. 39 we obtain Φ_0.

6. Duration of initiation

We can define two characteristic times in the system. The first one, a/c, is related to the wave velocity and the other one can be defined through the characteristic slip patch α^{-1} by $1/(c\alpha)$. For the infinite system size the latter is the only time scale we have and it gives the order of the duration of initiation T_c on an infinite fault (see Campillo and Ionescu [3] for an approximative formula of T_c). For a finite system size the duration of initiation does not scale with any of these two characteristic times. Indeed, as follows from the numerical experiments of Ionescu and Campillo [10], the duration of initiation becomes very large when the fault length $2a$ approaches the critical value $2a_c$. In this section we explain this behavior through the stability analysis presented above.

Here, we use the expression of the dominant part w^d to find an approximate formula for T_c, the duration of the initiation phase. Since the evolution of the slip $w(t,x,0+)$ is in essence described by the dominant part, T_c satisfies $\sup_{x\in R} w^d(T_c,x,0+) = L_c$. Assuming that the initial perturbation is such that the first point x of the fault for which the slip reaches the critical value L_c is $x=0$, we obtain that T_c is the solution of the equation $w^d(T_c,0,0+) = L_c$.

Let us suppose in what follows that:

$$1.1577\ldots = \beta_0 < \beta = a\frac{(\mu_s-\mu_d)S}{GL_c} < \beta_1 = 2.754\ldots$$

i.e. we deal with one eigenfunction in the expression of the dominant part w^d. This case corresponds to 'long' initiation periods for which λ_0 is small.

If we note $A_0 = \Phi_0(0,0+)$ then from Eq. 23 we obtain:

$$L_c \approx A_0\left[\cosh(c\lambda_0 T_c/a)W_0^0 + a\frac{\sinh(c\lambda_0 T_c/a)}{c\lambda_0}W_0^1\right]$$

where W_0^0 and W_0^1 are the weighted averages of the initial perturbation given by Eq. 22. More precisely they are the projection of w_0, w_1 on the first eigenfunction Φ_0. One can use the above equation to deduce the following approximate formula for T_c:

$$T_c \approx \frac{a}{c\lambda_0}\ln\left[\frac{c\lambda_0 L_c/A_0 + \sqrt{c\lambda_0 L_c/A_0)^2 - (\lambda_0 c W_0^0)^2 + (aW_0^1)^2}}{\lambda_0 c W_0^0 + aW_0^1}\right] \quad (42)$$

We remark that T_c depends on the initial averages W_0 and W_1 through a natural logarithm, hence the duration of the initiation phase has only a weak (logarithmic) dependence on the amplitude of the initial perturbation.

The duration of the initiation T_c also depends on the nondimensional weakening rate β through the functions $\lambda_0(\beta)$ and $A_0(\beta)$. Noticing that for $\beta \to \beta_0$, with $\beta > \beta_0$, we have $\lambda_0(\beta) \to 0$ and therefore $T_c \to +\infty$. That is when approaching the critical value β_0 the system has a slow unstable behavior.

The above formula is valid only for a linear dependence of the friction coefficient μ on the slip u in the weakening domain ($u \in [0,L_c]$ in our case). If a nonlinear weakening dependence $\mu = \mu(u)$ is considered, much slower evolution of the initiation phase can be expected in the neighborhood of the slip u_0 for which $\mu'(u_0) = 0$.

7. Numerical results

The theoretical development in the previous sections indicates some strong and simple properties of the slip during the initiation phase. In particular, the essence of the system evolution is described by the simple expression in Eq. 23 which we refer to as the dominant part. The aim of this

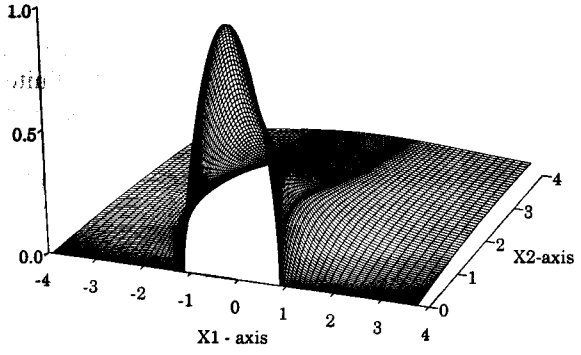

Fig. 2. First eigenfunction $\Phi_0(x_1,x_2)$ computed for $\beta=1.1764$ (which corresponds to $\lambda_0=0.1$) as a function of nondimensional variables $x_1=x/a, x_2=y/a$. It gives the spatial behavior of the dominant part.

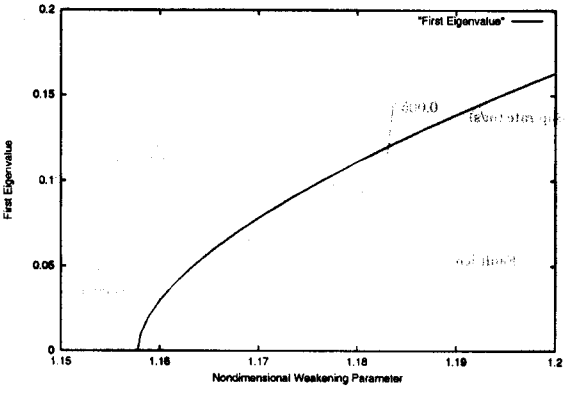

Fig. 4. The computed value of the first eigenvalue $\lambda_0=\lambda_0(\beta)$ versus the nondimensional weakening rate β. The intersection with the β-axis is the critical value β_0.

section is to compute the leading part. These results are then compared with the fully nonlinear solution computed with a finite difference scheme.

We have numerically solved the nondimensional eigenvalue problem (Eqs. 17–19) by truncation of the series in Eq. 40 up to $M=100$ terms. As in the static case, it was observed that such a truncation gives a high level of accuracy for the discrete solution. In Fig. 2 we plotted the first eigenfunction Φ_0 computed for $\beta=1.1764$ which corresponds to $\lambda_0=0.1$. It was obtained from Eq. 63 by discretization of the integral through a Gaussian quadrature. We remark that the eigenfunction is rather concentrated on the fault. We have also computed the partial derivative $\partial_{x2}\Phi_0$ (see Fig. 3), which gives the variation of the tangential stress acting on the fault. To do this we have employed Eq. 64 with the same numerical approach as for Φ. Fig. 3 illustrates the infinite limit of the outside tangential stress at the ends of the fault.

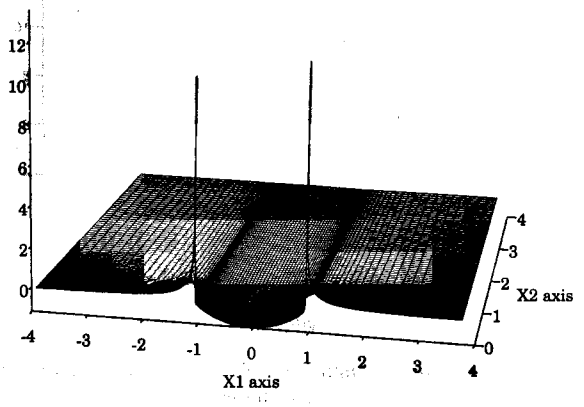

Fig. 3. Partial derivative $\partial_{x_2}\Phi_0(x_1,x_2)$ of the first eigenfunction computed for $\beta=1.1764$ (which corresponds to $\lambda_0=0.1$) as a function of nondimensional variables $x_1=x/a, x_2=y/a$. It gives the spatial behavior of the tangential stress σ_{yz}. Note the stress singularities at the ends of the fault.

In Fig. 4 we have plotted the first eigenvalue λ_0 as a function of the nondimensional parameter β. We note a significant increase of the eigenvalue in the neighborhood of $\beta_0=1.1577...$, the intersection of the graphic with the β-axis.

The following numerical results were obtained using a finite-differences scheme proposed by Ionescu and Campillo [10] to approach the nonlinear problem (Eqs. 1–5). We used a grid of 800×800 points in the x,y plane and the following model parameters: $\rho=3000$ kg/m^3, $c=3000$ m/s, $\mu_s=0.8$ and $\mu_d=0.72$ and the half length of the fault is $a=500$ m. The normal stress is assumed to correspond to a lithostatic pressure corresponding to a depth of 5 km. The initial condition corresponds to a velocity perturbation w_1 while the initial displacement perturbation w_0 is 0.

The initial velocity perturbation has the following distribution:

$$w_1(x,y)=A\exp\left(\frac{(x-x_0)^2}{(x-x_0)^2-h^2}\right)\cos(\pi y/(2h)),$$

$$|x-x_0|<h,\ |y|<h,\ w_1(x,y)=0 \text{ elsewhere} \tag{43}$$

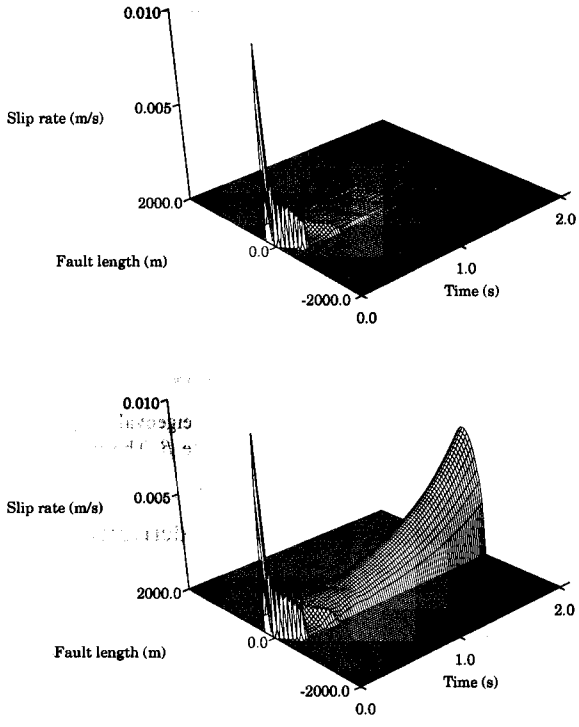

Fig. 5. Slip velocity ($\partial_t \delta w(t,x)$) on the fault ($y=0$) as a function of space x and time t computed with a finite-differences method. Here the half length of the fault is $a=500$ m. In the upper part of the figure $\beta=1.1<\beta_0$ (i.e. $L_c=19.8$ cm) and in the lower part $\beta=1.2>\beta_0$ (i.e. $L_c=18.1$ cm). Note the qualitatively different behavior with the same initial perturbation.

where the half width h is 100 m, the maximum amplitude A is 0.01 m/s.

In order to illustrate the stability analysis, given in Section 3, we show in Fig. 5 the evolution of the slip rate on the fault for $\beta=1.1<\beta_0$ (Fig. 5, upper part) and for $\beta=1.2>\beta_0$ (Fig. 5, lower part). We note the qualitatively different behavior of the solution in the two cases for a small variation of L_c ($L_c=19.8$ cm in the first case and $L_c=18.1$ cm in the second case). Indeed we see that after propagation and reflection on the end points of the fault, the initial perturbation vanishes in the first case but it has an exponential growth in the second case.

In Fig. 6 we have represented the duration of the initiation T_c given by Eq. 42 versus the coefficient β, for $a=500$ m and $c=3000$ m/s and using the computed value of $\Phi(0,0+)$. Note that for β approaching β_0 the duration of initiation, T_c, becomes infinite. In Fig. 6 we have also plotted the duration of the initiation obtained by the finite-differences computation of the dynamic solution. These results on the duration were deduced for different values of the critical slip L_c by keeping all the other physical values fixed, i.e. for different values of the nondimensional weakening rate β. The values of λ_0 in Eq. 42 are computed using the approach presented in Section 5 which is valid for small values of λ, i.e. for great T_c. On the other hand the finite-differences scheme can be applied on small intervals of time (consequence of the Courant–Friedrichs–Lewy condition). Nevertheless we note a rather good agreement between the numerical results obtained with the two methods.

8. Conclusions

To investigate the parameters which control the delay of triggering, we studied the initiation of slip instabilities of a finite fault in a homogeneous

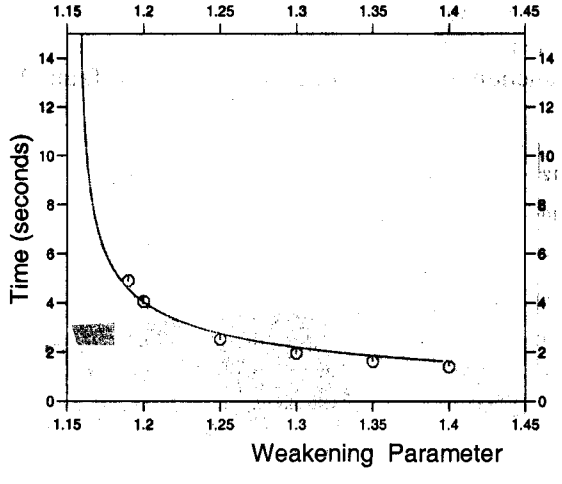

Fig. 6. Duration of initiation T_c versus nondimensional weakening coefficient β, for $a=500$ m and $c=3000$ m/s computed from Eq. 42 (continuous line) and obtained after the finite-differences computation of the dynamic solution (circles). Note the good agreement between these results. For β approaching β_0 the duration of initiation T_c becomes infinite.

linear elastic space. We considered the antiplane unstable shearing under a slip-dependent friction law with a constant weakening rate. The problem was attacked by spectral analysis. We concentrated our attention on the case of long initiation, i.e. small positive eigenvalues. A static analysis of stability was presented for the nondimensional problem. Using an integral equation method the first (nondimensional) eigenvalue, which depends only on the geometry of the problem, was determined. In connection with the weakening rate and the fault length this (universal) constant determines the range of instability for the dynamic problem. An accurate limiting value of the length of an unstable fault for a given friction law was given. By means of a spectral expansion, the 'dominant part' of the unstable dynamic solution was defined. It characterizes the exponential time growth. For the long-term evolution of the initiation phase the dynamic eigenvalue problem was reduced to a hypersingular integral equation. The expression of the dominant part was used to deduce an approximate formula for the duration of the initiation phase. The first eigenfunction was obtained numerically. The dependence of the first eigenvalue and the duration of the initiation on the weakening rate were pointed out. The results were compared with those for the full solution computed with a finite-differences scheme. These results suggest that a very simple friction law could imply a broad range of duration of initiation. They show the fundamental role played by the limited extent of the potentially slipping patch in the triggering of an unstable rupture event. This point is absent from the numerous discussions of the triggering process based on spring slider systems or infinite fault models, making their conclusions regarding the state of stress on the faults or the acceptable friction laws highly questionable.

Acknowledgements

We thank A. Cochard, J.-P. Vilotte, and an anonymous reviewer for their comments and their suggestions to improve this paper. This work was partially supported by the program MIG of Université de Savoie and by GDR 'FORPRO' (Action 98 A). C.D. was supported by Rhône-Alpes Region, grant TEMPRA-PECO.*[FA]*

Appendix A. Static eigenvalue problem

In the following, we give some details of the calculus for the static eigenvalue problem (Eqs. 25–27) of Section 4. The Fourier transform in x_1 of Eq. 25 leads to:

$$\frac{\partial^2 \hat{\varphi}}{\partial x_2^2} \xi^2 \hat{\varphi} \tag{44}$$

where $\varphi(\xi,x_2)$ is the Fourier transform in x_1 of $\varphi(x_1,x_2)$. The finite-energy solutions of Eq. 44, which require that $\nabla\varphi$ is vanishing at infinity, have the form:

$$\hat{\varphi}(\xi, x_2) = A(\xi) e^{-|\xi| x_2} \tag{45}$$

The Fourier inverse of Eq. 45 is:

$$\varphi(x_1, x_2) = \frac{1}{2\pi} \int_{-\infty}^{+\infty} A(\xi) e^{-|\xi| x_2 - i\xi x_1} \mathrm{d}\xi \tag{46}$$

and for $x_2 = 0$ it leads to:

$$A(\xi) = \int_{-\infty}^{+\infty} \varphi(s,0) e^{i\xi s} \mathrm{d}s \tag{47}$$

By substitution of $A(\xi)$ in Eq. 46 and interchange of the integration order we get:

$$\varphi(x_1, x_2) = \frac{x_2}{\pi} \int_{-1}^{1} \frac{\varphi(s,0)}{x_2^2 + (s - x_1)^2} \mathrm{d}s \tag{48}$$

which is a representation formula for the displacement field $\varphi(x_1,x_2)$. To deduce Eq. 48 we have used the relation

$$\int_0^{+\infty} e^{-\xi x_2} \cos(\xi(s - x_1)) \mathrm{d}\xi = \frac{x_2}{x_2^2 + (s - x_1)^2}$$

(see [2], ch. 1.4). By derivation with respect to x_2

we obtain:

$$\frac{\partial \varphi}{\partial x_2}(x_1,x_2)=\frac{1}{\pi}\int_{-1}^{1}\varphi(s,0)\frac{(s-x_1)^2-x_2^2}{(x_2^2+(s-x_1)^2)^2}\mathrm{d}s \quad (49)$$

which, for $x_2=0$, gives:

$$\frac{\partial \varphi}{\partial x_2}(x_1,0)=\frac{1}{\pi}FP\int_{-1}^{1}\frac{\varphi(s,0)}{(s-x_1)^2}\mathrm{d}s \quad (50)$$

where the integral is taken in the finite part sense.

For $x_1\in(-1,1)$, from the boundary condition (Eq. 27), we have:

$$\varphi(x_1,0)=-\frac{1}{\beta\pi}FP\int_{-1}^{1}\frac{\varphi(s,0)}{(s-x_1)^2}\mathrm{d}s \quad (51)$$

which is a hypersingular integral equation for $\varphi(x_1,0)$, $x_1\in(-1,1)$. After integration by parts Eq. 51 can be written as:

$$\varphi(x_1,0)=\frac{1}{\beta\pi}PV\int_{-1}^{1}\frac{\partial_s\varphi(s,0)}{x_1-s}\mathrm{d}s,\ |x_1|<1 \quad (52)$$

where the integral is taken in the Cauchy principal value sense. To solve Eq. 52) we seek a solution of the form of Eq. 31. Introducing $x_1=\cos\theta$, $s=\cos\psi$ and substituting Eq. 31 in Eq. 52, we obtain:

$$\pi\beta\sum_{n=1}^{\infty}u_n\sin(n\theta)=$$

$$\sum_{n=1}^{\infty}nu_n\int_0^{\pi}\frac{\cos(n\psi)d\psi}{\cos\psi-\cos\theta},\ \theta\in(0,\pi) \quad (53)$$

The Glauert integral formula:

$$\int_0^{\pi}\frac{\cos(n\psi)d\psi}{\cos\psi-\cos\theta}=\pi\frac{\sin(n\theta)}{\sin\theta} \quad (54)$$

reduces Eq. 53 to:

$$\beta\sum_{n=1}^{\infty}u_n\sin(n\theta)=\sum_{n=1}^{\infty}nu_n\frac{\sin(n\theta)}{\sin\theta} \quad (55)$$

for $\theta\in(0,\pi)$. Multiplication of this equation with $\sin(k\theta)\sin\theta$ and integration on $(0,\pi)$ yields:

$$\beta\sum_{n=1}^{\infty}A_{kn}u_n=\sum_{n=1}^{\infty}B_{kn}u_n,\ k=1,2,\ldots \quad (56)$$

where:

$$A_{kn}=\int_0^{\pi}\sin(n\theta)\sin(k\theta)\sin\theta d\theta=$$

$$-\frac{2kn(1+(-1)^{k+n})}{((k-n)^2-1)((k+n)^2-1)}(1-\delta_{n,k-1})(1-\delta_{n,k+1}) \quad (57)$$

$$B_{kn}=n\int_0^{\pi}\sin(n\theta)\sin(k\theta)\mathrm{d}\theta=\frac{n\pi}{2}\delta_{k,n} \quad (58)$$

Appendix B. Dynamic eigenvalue problem

In this Appendix we develop the mathematical approach of the dynamic eigenvalue problem (Eqs. 17–19) presented in Section 3. By Fourier transform in x_1 of Eq. 17 we get:

$$\frac{\partial^2\hat{\Phi}}{\partial x_2^2}=(\xi^2+\lambda^2)\hat{\Phi} \quad (59)$$

For $x_2>0$ the finite-energy solution of Eq. 59 is:

$$\hat{\Phi}(\xi,x_2)=A(\xi)e^{-\sqrt{\xi^2+\lambda^2}x_2} \quad (60)$$

Its Fourier inverse is:

$$\Phi(x_1,x_2)=\frac{1}{2\pi}\int_{-\infty}^{+\infty}A(\xi)e^{-\sqrt{\xi^2+\lambda^2}x_2-i\xi x_1}\mathrm{d}\xi \quad (61)$$

which, for $x_2=0$, yields:

$$A(\xi)=\int_{-1}^{1}\Phi(t,0)e^{i\xi t}\mathrm{d}t \quad (62)$$

When this expression of $A(\xi)$ is substituted in Eq. 61 and using the formula (see [2]):

$$\int_0^\infty e^{-x_2\sqrt{\lambda^2+\xi^2}}\cos(\xi(s-x_1))\mathrm{d}\xi =$$

$$\frac{|\lambda|x_2}{\sqrt{x_2^2+(s-x_1)^2}}K_1\left(|\lambda|\sqrt{x_2^2+(s-x_1)^2}\right)$$

we find:

$$\Phi(x_1,x_2)\frac{1}{2\pi}\int_{-1}^{1}\Phi(s,0)\int_{-\infty}^{+\infty}e^{-\sqrt{\xi^2+\lambda^2}x_2-i\xi(x_1-s)}\mathrm{d}\xi\,\mathrm{d}s =$$

$$\frac{|\lambda|x_2}{\pi}\int_{-1}^{1}\Phi(s,0)\frac{K_1(|\lambda|\sqrt{x_2^2+(s-x_1)^2})}{\sqrt{x_2^2+(s-x_1)^2}}\mathrm{d}s \tag{63}$$

with K_1 being the modified Bessel function of the second kind. This formula is the representation of the displacements in the upper half plane. By taking the derivative with respect to x_2 we have:

$$\frac{\partial\Phi}{\partial x_2}(x_1,x_2)=\frac{|\lambda|}{\pi}\int_{-1}^{1}\Phi(s,0)\Lambda(s,x_1,x_2)\mathrm{d}s \tag{64}$$

where:

$$\Lambda(s,x_1,x_2)=\frac{((s-x_1)^2-x_2^2)K_1(|\lambda|)\sqrt{x_2^2+(s-x_1)^2}}{((s-x_1)^2+x_2^2)\sqrt{x_2^2+(s-x_1)^2}}-$$

$$\frac{|\lambda|x_2^2K_0(|\lambda|\sqrt{x_2^2+(s-x_1)^2})}{(s-x_1)^2+x_2^2} \tag{65}$$

For $x_2\to 0$ from Eqs. 64 and 65 we find:

$$\frac{\partial\Phi}{\partial x_2}(x_1,0)=\frac{|\lambda|}{\pi}FP\int_{-1}^{1}\Phi(s,0)\frac{K_1(|\lambda(s-x_1)|)}{|s-x_1|}\mathrm{d}s \tag{66}$$

The boundary condition (Eq. 19) yields:

$$\Phi(x_1,0)=$$

$$-\frac{|\lambda|}{\pi\beta}FP\int_{-1}^{1}\Phi(s,0)\frac{K_1(|\lambda(s-x_1)|)}{|s-x_1|}\mathrm{d}s,\ |x_1|<1 \tag{67}$$

which is a hypersingular integral equation for $\Phi(x_1,0)$ on $(-1,1)$. Integrating by parts and using the relations:

$$K'_0(x_1)=-K_1(x_1);\ K'_1(x_1)=-\frac{1}{x_1}K_1(x_1)-K_0(x_1) \tag{68}$$

with the prime meaning the derivative, we obtain from Eq. 67:

$$\pi\beta\Phi(x_1,0)=$$

$$PV\int_{-1}^{1}\partial_s\Phi(s,0)\frac{|\lambda(x_1-s)|K_1(|\lambda(s-x_1)|)}{x_1-s}\mathrm{d}s+$$

$$\lambda^2\int_{-1}^{1}\Phi(s,0)K_0(|\lambda(x_1-s)|)\mathrm{d}s \tag{69}$$

For small values of $|\lambda|$ (i.e. $|\lambda|\ll 1$), we can approximate:

$$K_0(x_1)\approx-\ln(x_1),\ K_1(x_1)\approx\frac{1}{x_1}$$

so that Eq. 69 becomes:

$$\pi\beta\Phi(x_1,0)=$$

$$PV\int_{-1}^{1}\frac{\partial_s\Phi(s,0)}{x_1-s}\mathrm{d}s-\lambda^2\int_{-1}^{1}\Phi(s,0)\ln(|\lambda(s-x_1)|)\mathrm{d}s \tag{70}$$

for $|x_1|<1$. To solve Eq. 70 we use the same technique as in Appendix A. We seek a solution for Eq. 70 of the form of Eq. 39. In this case the

infinite system corresponding to Eq. 56 is:

$$\beta\sum_{n=1}^{\infty}A_{kn}U_n=\sum_{n=1}^{\infty}(B_{kn}+C_{kn}(\lambda))U_n,\ k=1,2,\ldots \tag{71}$$

with A_{kn},B_{kn} given by Eqs. 57 and 58 and:

$$C_{kn}(\lambda)=-\frac{\lambda^2}{\pi}\int_0^{\pi}\int_0^{\pi}\sin(k\theta)\sin(n\varphi)\sin\theta\sin\varphi\ln$$

$$(\lambda|\cos\theta-\cos\varphi|)\mathrm{d}\varphi\mathrm{d}\theta=\frac{\pi\lambda^2\ln\psi\lambda}{4}\delta_{n,1}\delta_{k,1}$$

$$-\frac{\pi\lambda^2}{16}(\delta_{k,3}-(1+4\ln 2)\delta_{k,1})\delta_{n,1}$$

$$-\frac{\pi\lambda^2}{8(n^2-1)}(1-\delta_{n,3})$$

$$[(n-1)\delta_{k,n+2}+(n+1)\delta_{k,n-2}-2n\delta_{k,n}] \tag{72}$$

References

[1] D.J. Andrews, Rupture propagation with finite stress in antiplane strain, J. Geophys. Res. 81 (1976) 3575–3582.

[2] A. Erdélyi, W. Magnus, F. Oberhettinger, F.G. Tricomi, Tables of Integral Transforms, Bateman Manuscript Project, MacGraw-Hill, New York, 1954.

[3] M. Campillo, I.R. Ionescu, Initiation of antiplane shear instability under slip dependent friction, J. Geophys. Res. 102 (B9) (1997) 20363–20371.

[4] L. Dragos, Method of fundamental solutions. A novel theory of lifting surface in a subsonic flow, Arch. Mech. 35 (1983) 575.

[5] L. Dragos, Integration of Prandtl's equation with the aid of quadrature formulae of Gauss type, Q. Appl. Math. 52 (1994) 23–29.

[6] W.L. Ellsworth, G.C. Beroza, Seismic evidence for an earthquake nucleation phase, Science 268 (1995) 851–855.

[7] Ch. Fox, A generalisation of the Cauchy principal value, Can. J. Math. 9 (1957) 110.

[8] R.A. Harris, Introduction to special section: Stress triggers, stress shadows, and implications for seismic hazard, J. Geophys. Res. 103 (1998) 24347–24358.

[9] Y. Iio, Slow initial phase of the P-wave velocity pulse generated by microearthquakes, Geophys. Res. Lett. 19 (1992) 477–480.

[10] I.R. Ionescu, M. Campillo, Influence of the shape of the friction law and fault finiteness on the duration of initiation, J. Geophys. Res. 104 (B2) (1999) 3013–3024.

[11] I.R. Ionescu, J.-C. Paumier, On the contact problem with slip dependent friction in elastostatics, Int. J. Eng. Sci. 34 (1996) 471–491.

[12] M. Ohnaka, Nonuniformity of the constitutive law parameters for shear rupture and quasistatic nucleation to dynamic rupture: A physical model of earthquake generation model, Paper Presented at Earthquake Prediction: The Scientific Challenge, US Acad. Sci., Irvine, CA, 1996.

[13] A.C. Palmer, J.R. Rice, The growth of slip surfaces in the progressive failure of over consolidated clay, Proc. R. Soc. London A 332 (1973) 527–548.

[14] J.E. Vidale, D. Carr Agnew, M.J.S. Johnston, D.H. Oppenheimer, Absence of earthquake correlation with earth tides: an indication of high preseismic fault stress rate, J. Geophys. Res. 103 (1998) 24567–24572.